Saturation Power Tolerance Studies for the Linac Coherent Light Source

Matthew Anderson*
Department of Physics, University of California, Los Angeles
(Dated: October 12, 2003)

We examine the power output tolerance of a simulated version of the Linac Coherent Light Source (LCLS). We study the power output variation from optimal with independent variation in undulator field strength and undulator offsets. Our simulations suggest a tolerance of 0.1% percent for undulator field strength and 50 μm tolerance in undulator offset.

INTRODUCTION

The Linac Coherent Light Source is being constructed at the Stanford Linear Acceleration with a projected start of operations in 2008. A number of studies have been initiated for the for the purposes of determining the engineering specifications and tolerances for the fully built machine. This paper takes up a small part of the larger issue; examining the necessary tolerances for magnetic field strength errors and errors in undulator longitudinal placement. We use a method of computer simulation to examine these effects because the construction of a physical copy of the LCLS would be a necessarily cyclic endeavor.

FEL BASICS

The LCLS Free Electron Laser (FEL) is a means to produce a high-brightness X-ray laser pulse[1]. The lasing action of the FEL is analogous to the stimulated emission process in a gas or solid state laser. The lasing medium in the FEL is an ultra-relativistic, low-divergence beam of electrons[2, 3]. It is a process analogous to the quantum laser; the emission is due to the transition of electrons between unbound states in its interaction with a magnetic field. The beam passes, in the z-direction, through a series of magnets called "undulators". These undulators consist of small dipole magnets of alternating polarity that maintain a magnetic field in the y-direction, perpendicular to the path of the electrons, of the form

$$B_y = B_0 \cos k_u z, \tag{1}$$

where B_y is the strength of the y-component of the magnetic field on axis, B_0 is total amplitude of the magnetic field, k_u is wave number corresponding the period of the undulator magnets, and z is the displacement along the undulator axis. The alternating fields cause the electron beam to oscillate in the x-direction, perpendicular to both the initial direction of motion and the magnetic field. A short undulator is diagrammed in figure 1. The electrons emit synchrotron radiation as they are deflected by the magnetic fields of the undulator[4]. Only radiation emitted at a certain frequency, and those of its higher harmonics, will resonate in the undulator. A FEL can operate with a single long undulator, but it is usually split up into several modules for beam diagnostics, focusing and pumping. The modules act in tandem to produce a laser pulse at the resonant frequency. Drift sections between undulator modules contain diagnostic equipment for monitoring the output radiation and electron beam. Quadrupole magnets may also be placed in these regions to allow for focusing of electron beam in either x- or y-planes and to keep the electron density high. This focusing keeps the size of the electron beam small. Steering magnets known as "correctors" may be placed in these regions to correct for the kick in momentum the electrons receive from the fringe fields of the undulator or misaligned quadrupoles.

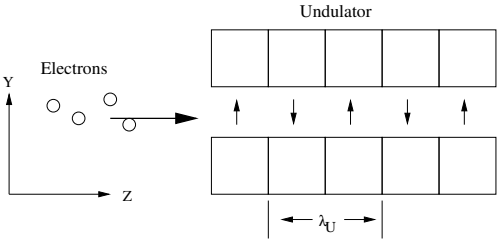

FIG. 1: Simple Diagram of Undulator Module: *electrons enter from the left at high velocity in the z-direction*

There is an energy exchange between the free electrons and the radiation field due to their transverse motion, which is given by

$$\frac{d\gamma}{dt} = \frac{e\vec{E}\cdot\vec{v}}{m_0 c}, \tag{2}$$

where $\frac{d\gamma}{dt}$ is the rate of change of electron energy versus time, $\vec{E}$ is the electric field vector for the radiation field at the position of the electron and $\vec{v}$ is the velocity of the electron, e is the charge of the electron, m_0 is the mass of the electron and c is the speed of light *in vacuo*. At the resonant frequency the energy change is constant and accumulates over many periods.

The resonance frequency of radiation depends on a number of parameters. The resonance wavelength is

Parameter	Value
FEL Length	120 m
γ	14.328 GeV
λ_0	1.505 Å
k_U	209 $\frac{rad}{m}$
Number of Undulator Modules	34
Length of Undulator Modules	3.36 m

FIG. 2: Simulation Parameter Values

given by the following resonance relation:

$$\lambda_0 = \frac{\lambda_U}{2\gamma^2}(1 + K^2), \tag{3}$$

λ_0 is the resonant wavelength of the FEL, λ_U is the period of the magnetic field. K is a dimensionless constant that is proportional to the strength and period of the undulator fields:

$$K = \frac{eB_0}{\sqrt{2}mck_U}. \tag{4}$$

Resonance occurs when the radiation advances one wavelength each undulator period. The magnetic field period and the magnetic field strength are constants of FEL apparatus. However, the energy of the incoming electrons, γ, can be altered to control the resonant frequency. Therefore, the FEL is tunable in contrast to the fixed frequency of the conventional quantum laser.

The motivation for this study is to determine the tolerable deviation from an ideal undulator in order set engineering limits. We use simulations to examined these tolerances because it would be impossible to solve the equations of motion in this inherently non-linear and coupled system.

A concise list of starting simulation parameters for LCLS are shown in figure 2.

The K parameter defined by eqn 4 is dependent on the RMS value for field strength and period averaged across all undulator modules. We see that λ_0 varies like the square of the field strength for large values of K. If there is sufficient error in magnetic field strength, that is, the deviation of the field strength from optimal is large, the resonance condition will become a function of longitudinal position, z.

We simulate errors in the magnetic field and observe how saturation (output) power of the FEL is affected. These simulations will help to get an estimate of the tolerable amount of relative variation in the LCLS FEL.

The simulations focused on two types of field errors: correlated and uncorrelated errors. Uncorrelated errors are simply random field variation around the calculated optimal field strength on each set of poles in the undulators. Correlated errors depend on the errors in adjacent regions for their values. Correlated errors attempt to minimize the first and second field integrals of the magnetic field, which are proportional to the net change in transverse (x-direction) momentum and position respectively. Having given the fundamental principles we proceed to several indicators of performance.

The "phase shake" of the interaction phase between the particles and the radiation field is defined as $\theta = (k + k_U)z - \omega t$. The phase shake is a measure of how far "out of phase" the electron beam is with respect to the radiation it is resonating with:

$$\theta_{PS}(z) = \int_0^z \frac{d\theta}{dz}dz - \bar{\theta}\frac{z}{L} = -\int_0^z (k+k_u)\frac{\beta_x^2 + \beta_y^2}{2}dz - \bar{\theta}\frac{z}{L}; \tag{5}$$

k is the wave number of the resonant radiation, k_u is the wave number corresponding to the period of the undulator magnets, β_x and β_y, respectively, are the average values of the x- and y-components of beam's velocity (in units of c). Because the LCLS undulator is planar, field errors do not excite a motion in x and therefore β_x can be assumed to be zero. We subtract $\bar{\theta}\frac{z}{L}$ where $\bar{\theta}$ is the slope from a linear fit to $\int_0^z \frac{d\theta}{dz}dz$, because any linear drift in interaction phase, θ, can be compensated for by adjusting the beam energy. θ_{PS} is the residual fluctuation around a constant phase. A "sudden" phase shake of π would put the electron beam completely out of phase with the radiation, causing it to emit radiation that destructively interferes with the radiation already propagating through the undulator. Whenever the phase shake is much different from zero, resonance suffers, reducing the output power of the free electron laser. While θ_{PS} can have both signs, a parameter for describing field quality is the rms value of θ_{PS}. A larger value of $\theta_{PS,rms}$ corresponds to a larger phase shake and, therefore, a stronger degradation of the FEL performance.

The value of K given in eqn 4 is an approximation for on axis K values; K also varies in both transverse directions (x- and y-directions)[5]:

$$K(x, y) = \frac{eB_0}{\sqrt{2}mck_U}(1 + \frac{k_x^2}{2}x^2 + \frac{k_y^2}{2}y^2), \tag{6}$$

where the values of k_x and k_y depend on magnet geometry and satisfy the pythagorean constraint with k_U, B_0 is the magnetic field at the center of the undulator, e is electron's charge. The value for K in equation 3 is the on-axis value of $K = K(0, 0)$. For LCLS the intended undulator geometry is planar with $k_x = 0$ and $k_y = k_U$, making the effective K only a function of the y-offset of the beam or undulator. The FEL performance is invariant to x-offsets.

All of this background material is discussed more completely in [6].

We will proceed first with a first of the tolerance of saturation power and length to field errors. The second discussion is of power tolerance to undulator offsets. All data was a result of 3-D numerical modelling using the

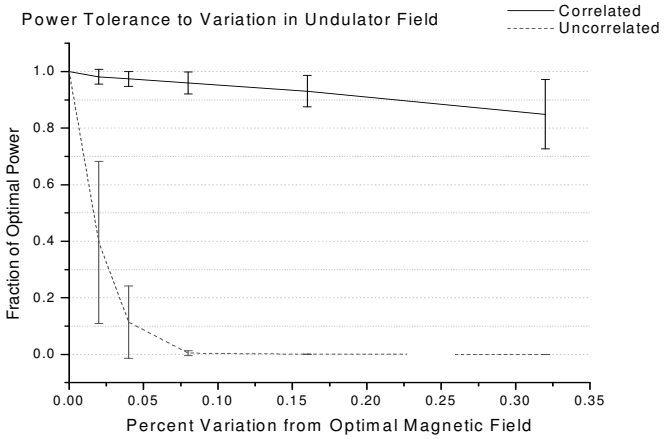

FIG. 3: Power Tolerance to Variation in Undulator fields

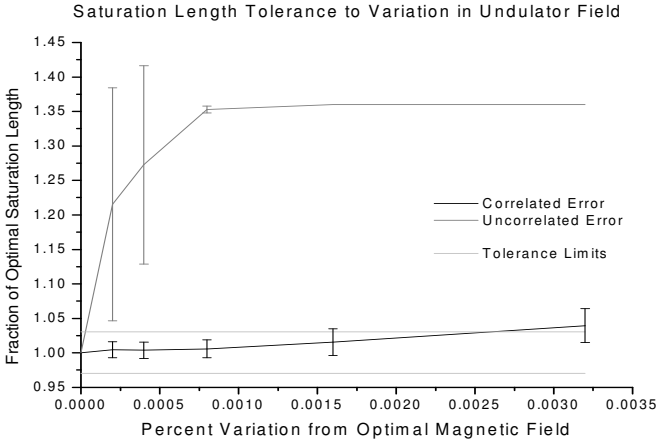

FIG. 4: Saturation Length Tolerance to Variation in Undulator Field

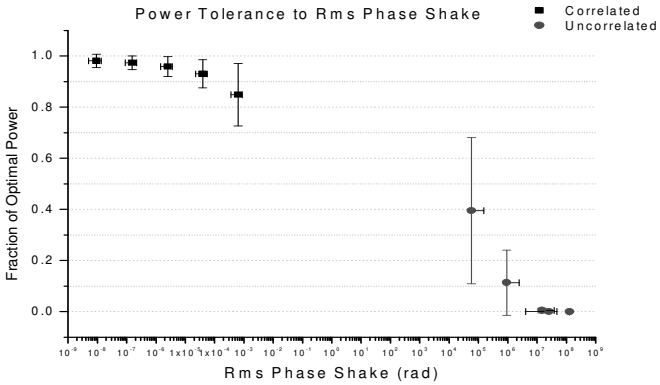

FIG. 5: Power Tolerance to Phase Shake

program *Genesis 1.3*[6]. *Genesis 1.3* simulates FEL behavior by numerical integrating the equations of motions for electrons traversing a virtual FEL. More detailed explanations can be found on *Genesis 1.3* website[7].

TOLERANCE UNDER UNDULATOR FIELD VARIATIONS

We introduced errors in the magnetic field strength for both poles in each period of the undulators, λ_U, about the optimal (non-error) value and examined indicators of FEL performance, mainly saturation power and saturation length. We compared these indicators with several quantities such as the 1^{st} and 2^{nd} field integrals, and the value of the root-mean-square phase shake.

Field errors are generated between 0.02% to 0.32% rms fluctuation. The results are shown in figure 3. The data is normalized to the value of power without errors. Each data point on the figure is an average of nine runs with different random seeds. The error bars of each point is simply the standard deviation of each set of runs. Clearly, when the errors are uncorrelated, the power output scales poorly.

It is reasonable to assume that the actual type of error in the physical LCLS can be made to be correlated. The magnets of the undulator modules can be shimed, swapped and moved to a nearly optimal configuration, based on the errors of the set of magnets, can be obtained. For our purposes we will set the tolerance threshold at ninety percent of the optimal power output, which will give us an allowance of approximately 0.1% relative error in field of a given magnet (as shown in figure 3). Based on engineering estimates it is reasonable to assume that precision as good as 0.001% for uncorrelated errors can be achieved due to the limit of the precision for measuring magnetic field. Thus, there is no fundamental engineering obstacles to achieving necessary tolerances for good power output.

The saturation length is also a good indicator of performance. In figure 4. we plot relative saturation length versus maximum relative variation in field. The maximum relative saturation length is limited to 1.36 because the FEL we simulated is 120 meters long. For uncorrelated errors the amplitude of fluctuation about value when it is optimally configured is several orders of magnitude greater than the in the correlated case, which is nearly flat.

We will use the same tolerance threshold as the LCLS Conceptual Design Report (CDR)[1], which uses a 3% variation in saturation length as an appropriate tolerance threshold. The tolerance thresholds are shown on the graph for scale. Following the same arguments in the previous section, we can choose the tolerance to be about 0.1% and still be within 3% of the saturation length. This agrees with the result of the previous section with the choice of power tolerance threshold of 90%.

We examined how the power varies as a function of $\Delta\theta_{RMS,PS}$. In figure 5 we show the difference between relative saturation power and the value of the RMS phase shake. The uncertainty on the points is again the standard deviation of the set from the mean of the set. We

see that RMS phase shake is a good indicator of performance. The runs with low phase shake had higher output power. This makes sense because if there is a large phase difference the resonance ceases to occur and the output power is diminished. This result suggests that RMS phase shake is a universal variable regardless of the distinction between correlated and uncorrelated errors. Phase shake is also an essentially measurable quantity (dependent on the magnetic fields), so phase shake can be used, over preference for error type, as something that is "partially-correlated" error is ill-defined. We can assume that the data in figure 5 are two parts of the same function. This allows us to drop the distinction between the error types.

The graph also shows that the phase shake increases as relative error of the undulator field increases (the data points are in the same order as in figure 3). From the graph we see that we are allowed a phase shake as great as 10^{-5} radians over the course of the FEL and still maintain ninety percent of output power. It has little independent meaning, as the phase shake is a dependent variable; it, like saturation power depends on a large number of parameters. However, there is likely a less complex relationship between phase shake and power than field variance and power.

Finally, we will look at the tolerance of saturation power to the second field integral. The form of the first and second field integrals are shown below:

$$\Delta p \propto \int_0^L B_y(z)dz, \tag{7}$$

$$\Delta x \propto \int_0^L \int_0^L B_y(z)dz, \tag{8}$$

where L is the length of the FEL. The first field integral gives the average change in momentum of beam between it across the length of the FEL. The second field integral gives the FEL offset position. The field integrals are parameters that are entirely depend on the undulator, therefore, they are measurable during construction and are the parameters for field optimization. The first and second field integrals are intimately related in that if the second field integral is small, the first must also be sufficiently small as well.

In figure 6 the relationship between the second field integral and the output power is shown. We see that lower 2^{nd} field integrals allows for more optimal saturation power. We also see that the 2^{nd} field integrals of the cases with correlated errors have smaller field integrals and greater output power. This is to be expected, the correlated errors are generated in a way that nearly optimizes the 2^{nd} field integral. This supports the idea that configuring the undulator magnets in a way that reduces the field integral will provide a sufficiently good tolerance, with enough headroom above the value achievable

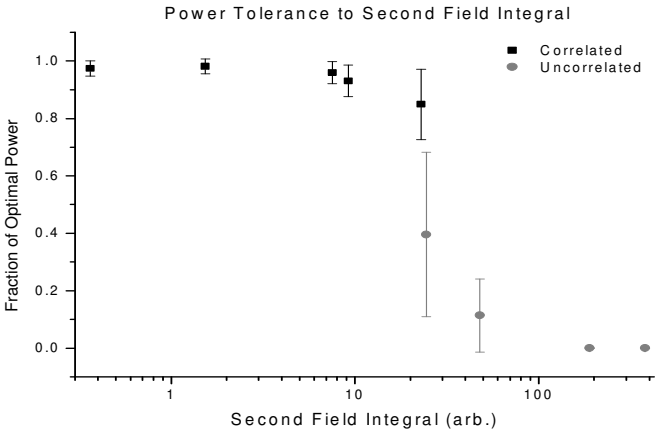

FIG. 6: Power Tolerance to 2^{nd} Field Integral

with reasonable engineering assumptions (a factor of one hundred). The graph also seems to suggest that the 2^{nd} field integral is another hidden variable that correlates error type and magnitude similarly to RMS phase shake; phase shake is dependent on the field integral. Minimizing power variation to field errors is tantamount to measuring and optimizing the 2^{nd} field integral.

TOLERANCE UNDER UNDULATOR Y-OFFSET VARIATIONS

We examine the tolerance output power to undulator y-offsets. Due to the planar configuration of the LCLS undulator, offset in x have no impact on the performance. We looked at uniformly random variation of undulator y-offset about a systematic offset. Four systematic offsets were used: 0, 50, 100, and 200 μm. In figure 7 we see the effect of changing the offset on the saturation power. All power calculations are normalized to the value at no offset and optimal power. The input energy of the electron beam is adjusted for each systematic offset to maximize the power, the optimized power is within 0.1% of the maximum power. We notice several things about this graph, the maximum output power decreases as the systematic offset increases. For undulator offsets, the undulator parameter K varies significantly over the transverse beam size to disturb the FEL resonance condition.

The effect is not linear, because it replaces y with (y - Δy) in equation 6, this results an addition to the equation determining K (equation 6). Thus K becomes larger in both absolute value and the magnitude of the variation off the minimum of the quadratic dependence. If K varies sufficiently along the axis of the FEL, the resonance condition (equation 3) also varies, and the effect is increased because because $\lambda_0 \propto K^2$. Therefore we also expect the runs with larger offsets and larger variations about the offset to drop in power more than ones with smaller offsets. Looking again at the graph and using

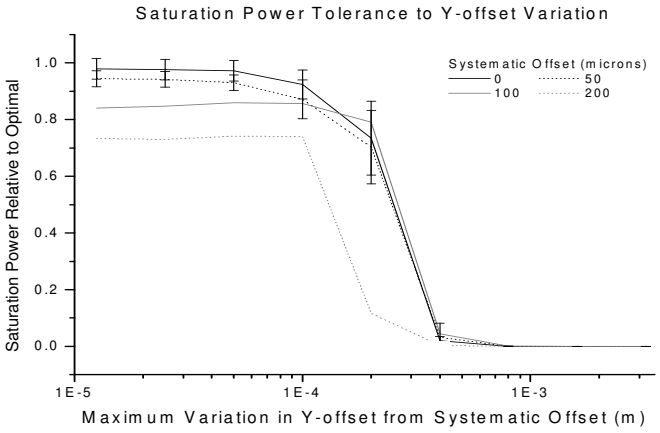

FIG. 7: Power Tolerance to Undulator Y-offset

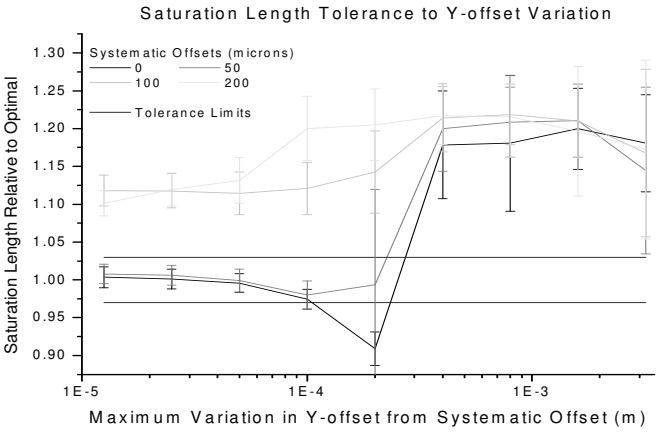

FIG. 8: Saturation Length Tolerance to Undulator Y-offset

our previous definition of tolerance, we observe that 90% power is still reached if we have a 50 μm systematic offset and a 50 μm uniform variation about the offset.

We can also looked the tolerance based on deviation from saturation length. In figure 8 we plot the saturation length versus amplitude of the uniform variation for the various undulator offsets. The uncertainty bars on this figure are again the standard deviation of the value in that set of runs, however, we only included the necessary uncertainties.

We see that the saturation length is closer to optimal when the offsets are small. The saturation length maximum value in the simulations is 120m, the length of the FEL, having longer saturation lengths would require a longer FEL. The maximum possible saturation length corresponds to approximately 1.24 times the optimal saturation length. Based on the 3% tolerance, we see that an appropriate choice for y-offset tolerance based on saturation length up to 50 μm systematic offset with an 50 μm variation about the systematic offset. This is coincidentally the tolerance that we also noted in the previous section. There is one point that has shorter saturation length than all the other for 0 micron systematic offset and 200 micron variations. This is likely because beam reached its saturation point near the interface between a drift section and an undulator making the subsequent trial miss there saturation because they were passing through a drift section.

CONCLUSION

We looked a two different undulator parameters that affect the output power of the LCLS FEL, undulator field errors and undulator offset errors. Using our simulations we suggest a tolerance of at least 0.1% percent for undulator field strength errors and for y-offset errors a 50 μm systematic offset with a 50 μm variation. This results are essentially consistent with the values quoted in the CDR, our explicit calculations agree with the CDR's rough analytic estimates[1]. These tolerances are technologically reasonable and achievable.

We have seen that two composite values, $\theta_{RMS,PS}$ and the 2^{nd} field integral, relate field error type and field error magnitude. Those values can be measured at the apparatus and optimized to reduce power losses to field errors as opposed to relying on the ill-defined error types "correlated" and "uncorrelated".

It is important to understand, however, that the simulations treated the variation in undulator field strength and undulator offset as each independently affecting the saturation power and length. In reality they are correlated, such that having both parameters at their separate tolerance limits(3%) would likely induce a variation different than 6% for saturation length. In fact, there are on the order of one hundred important parameters that are all correlated in a complicated fashion. It would be inherently difficult to search the many dimensional parameter space for the surface bounding the regions of tolerable performance.

FUTURE WORK

These tolerance values with be helpful in the construction of the LCLS, justifying reasonable engineering expectations and qualifying the original estimates made in the CDR. Future work should examine the results of a physical mockup of a section of undulator to similar variances in the field strength or undulator positioning. With the completion of the physical LCLS the true effects can be quantified and examined in relation to the results our simulations.

ACKNOWLEDGEMENTS

Thanks to the NSF for funding my research through the UCLA Physics REU Program. Thanks to Sven Reiche for advising my research and helping to unify the ideas in this paper. Thanks to Gil Travish for editing this paper, and finding me something else to do. Thanks to Francoise Queval for organizing this program.

* Electronic address: ma@andrew.cmu.edu; Department of Physics & School of Computer Science, Carnegie Mellon University, Pittsburgh

[1] LCLS - CDR SLAC-R-593, UC-414, SLAC (2002).
[2] J. Madey, J. App. Phys. **42** (1971).
[3] M. Cornacchia, Invited talk presented at SPIE Photonics West 99: Free-Electron Laser Challenges, San Jose, CA, USA LCLS-TN-99-6, SLAC (1999).
[4] J. Jackson, *Classical Electrodynamics* (John Wiley and Sons, 1999), 3rd ed.
[5] T. Scharlemann, J. App. Phys. **58** (1985).
[6] S. Reiche, Ph.D. thesis, University of Hamburg (1999).
[7] http://corona.physics.ucla.edu/ reiche/index.html